Scientific Research Publishing

Journal of Computer and Communications, 2026, 14(4), 181-200
https://www.scirp.org/journal/jcc
ISSN Online: 2327-5227
ISSN Print: 2327-5219

Left Hands or Right Hands? An Artificial Intelligence Method-Based Evidence for Finding Remote Ancient People's Habits When They Wrote Oracle Words that Were Deracinated 3000 Years Ago

Shichao Song, Xun Liang*, Zihuan Feng, Yang Xue

School of Information, Renmin University of China, Beijing, China
Email: *xliang@ruc.edu.cn

How to cite this paper: Song, S.C., Liang, X., Feng, Z.H. and Xue, Y. (2026) Left Hands or Right Hands? An Artificial Intelligence Method-Based Evidence for Finding Remote Ancient People's Habits When They Wrote Oracle Words that Were Deracinated 3000 Years Ago. *Journal of Computer and Communications*, **14**, 181-200.
https://doi.org/10.4236/jcc.2026.144009

Received: March 27, 2026
Accepted: April 25, 2026
Published: April 28, 2026

Abstract

Human beings like to ask where we came from and are always curious about how our habits evolved. One of our habits is handedness. It is found that cats and dogs do not differentiate between right- or left-handed forelimbs. But most humans are dextromanual. Did humans originate as dextromanual, or did most people converge to right-handedness as human society developed? To discover the answer, some archaeologists speculated that the ancients were right-handed because they found an ancient tooth fossil from 500,000 years ago in Spain skewed to the right. Is there more evidence? The extinct oracle bone scripts, written by ancient Chinese 3000 years ago, may expose some clues. We use the real images of the genuine rubbings provided by The Oracle Museum of China in our experiments. As it is well known, the power of deep learning networks has surpassed human beings in identifying subtle differences in images. Using the artificial intelligence tool, this paper studies the recognition of real oracle rubbings. Since it is impossible to recognize directly with the naked eye whether these rubbings were written by the left or right hand of ancient Chinese humans, this study has to employ the unsupervised method. We found through exhaustive experiments that the ancient oracle word authors were more likely to be dextromanual.

Keywords

Handedness Inference, Ancient Human Behavior, Oracle Bone Inscriptions, Shang Dynasty Writing

1. Introduction

The ancient Chinese oracle words, together with ancient Mayan characters and ancient cuneiform Sumerian characters, still tell profound historical mysteries for the modern world. The oracle rubbing words, engraved on the animal bones, were invented about 3000 years ago in the Shang Dynasty in China and were derived from. From then on, Chinese history entered an age recorded with written oracle rubbing words. The oracle words are the foundation of the evolution and development of Chinese characters and are treated as one of the remarkable symbols of Chinese civilization.

Since the discovery of the first oracle bone inscription in 1899, over 100 years have passed. During this period, many animal bones with oracle bone inscriptions have been unearthed. Most of the inscriptions are records of divination by the royal family of the Shang Dynasty and mainly about weather, agriculture, hunting, and instruments. At present, there are more than 4000 different oracle bone characters that have been manually categorized, of which more than 1000 have been identified with their corresponding modern Chinese characters. As early hieroglyphics, glyph drawings are still an important feature. The people who engaged in calligraphy and engraving activities in ancient times were called Zhenren, specializing in divination [1]. Different Zhenren represent different historical periods of the Shang Dynasty. Zhenren is often used as an important criterion for judging the staging of different kings.

Given the lack of standardization of ancient oracle bone inscriptions, the structure and form of the same characters are not unified. Oracle bone inscriptions are characterized by many homonyms, complexity, and simplicity. Homonymy means the same character with different shapes. Figure 1 shows six oracle bone inscriptions of the character "bird". The writing style of oracle characters is highly arbitrary, presenting a difficulty in oracle character revaluation.

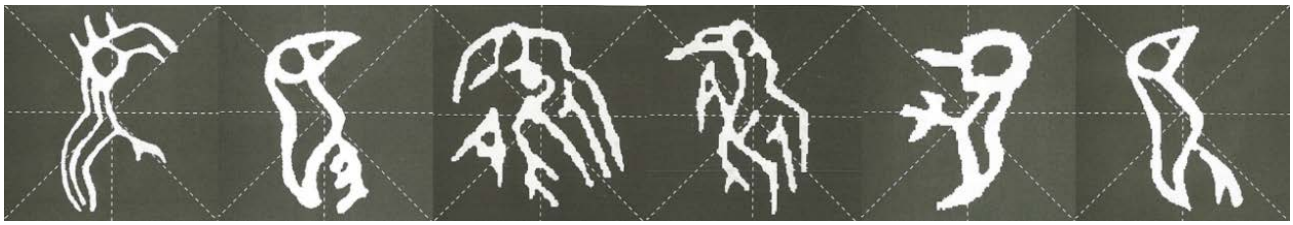

Figure 1. Different forms of the Chinese character "bird".

In the field of computer vision, an oracle is not only a character but also a picture. The writing style of oracle bone inscriptions is relatively free. Many kinds and configuration variations of oracle bone inscriptions exist, making the machine recognition of oracle bone inscriptions difficult. In addition to their homograph, complexity, combination, and pictograph characteristics, oracle bone inscriptions also have the characteristics of positive and negative coexistence, left-right symmetry, up and down symmetry, rotation, and change of meaning [2]. Oracle variant characters have a huge amount of noise for the traditional modern

character recognition process. Through computers and other means, we can recognize oracle variants and assist experts in completing the recognition and confirmation of oracle variants.

Our interest in oracle recognition stems from the question of whether humans originate as dextromanual, or most people converge to right-handedness as human society developed. Our main aim is to use the ability of deep learning to distinguish features in detail to investigate whether ancient humans were dextromanual or sinistromanual. David Phil, an anthropology professor at the University of Kansas, has studied ancient tools and human remains. He used the dents on the fossil incisors found in Spain as evidence that humans were right-handed 500,000 years ago. What's more, his colleagues in Croatia, Italy, and Spain have shown that the special traces on these fossil teeth are related to the right-handed or left-handed characteristics of prehistoric individuals. When people do a certain action, their hands and mouth will be very closely coordinated. When the stone tools are pulled, the tools accidentally scratch their lips, leaving these traces.

In daily life, we may find that there is no difference between dextromanual or sinistromanual forelimbs in cats and dogs, and their use of forelimbs is balanced. But studies have shown that upright gorillas have a preference for left and right hands [3] [4]. So dextromanuality may be an obvious feature of human beings [5]. Anthropological statistical analysis reveals that right-handed people outnumber left-handed people by a ratio of 9 to 1. The writing style of ancient writers of the mysterious oracle bone inscriptions thousands of years ago arouses interest. Through the naked eye, we cannot tell whether a certain oracle glyph was carved by the left or right hand of ancient humans. We hope to determine whether the authors of these oracles are dextromanual or sinistromanual through the ability of deep learning to identify features.

It is well known that in supervised learning, the accuracy given by a deep neural network in the field of image recognition is very high. For example, in face recognition, the recognition accuracy of machines exceeds that of humans. A person wearing a mask may not be recognized by friends, but can be recognized by a machine. The emergence of deep learning convolutional neural networks (CNNs) led to amazing progress in terms of recognition accuracy of 99%. In practice, labeling the data before the experiment is sometimes impossible. Oracle bone inscriptions that are still under study have no clear categorial labels. Thus, supervised machine learning is difficult to use for completing oracle revaluation. We need an unsupervised method to recognize oracle images.

Compared with high-precision supervised learning, unsupervised learning has lower learning precision because of its weak feature extraction ability. Due to the lack of annotation information, supervised learning is difficult to complete the fine-grained task of text image segmentation. In the research on ancient remote humans' oracle handwriting, because rubbing image data cannot be labeled as left- or right-hand, using unsupervised learning for left- and right-hand classification

is a necessary approach.

In the semantics task, words with similar context have similar semantics. Based on this, we believe that the adjacent pixels in the image also have similar meanings. Therefore, we regard each pixel in the oracle bone image as a word in the text. This method can read the oracle bone image in the form of text and map it to the high-dimensional feature vector, which provides a new idea for the application of deep mining unsupervised learning in fine-grained classification.

Inspired by the distribution hypothesis, this paper proposes an unsupervised oracle bone image revaluation algorithm to divide the unlabeled oracle bone image dataset to determine whether ancient people were sinistromanual or dextromanual. We presented a Bone2Vec method in this paper by embedding oracle images into a vector through deep learning. The experiments demonstrated that our proposed method gave the highest accuracy currently in unsupervised oracle hand preference identification.

Our main contributions are as follows:

1) We have manually scanned and processed all the available genuine oracle bone inscription images that have been recognized so far, containing more than 1000 recognized oracle bone images, and constructed the largest genuine oracle bone inscriptions dataset used in the research field of computer technology at present.

2) We proposed a Bone2Vec model that extracts the horizontal and vertical features of the image from the image pixels and uses a completely unsupervised algorithm for image embedding and clustering. Our model can also be used for other purposes as long as there is a strong correlation between the local data of the images. This model can be used to identify all the data without annotation information, such as handwriting identification in judicial expertise, true and false identification of calligraphy and painting, text age judgment, etc.

3) Archaeologists found evidence of left and right hands from ancient teeth, and the research on the left and right hands of oracle bone inscriptions provides new evidence for anthropological research from the perspective of computer technology.

2. Literature Review

The scope of oracle bone inscriptions research is extensive. In the traditional literature, only oracle experts can competently recognize oracle characters. The confirmation of oracle characters must be studied in many aspects. The common goal of all basic research works is to interpret more deciphered oracle bone inscriptions to unravel the history and culture of the Shang Dynasty 3000 years ago.

In the field of linguistics, oracle bone inscriptions are glyph drawings and the rudiment of the modern Chinese character system. In the field of computer science, Li and Zhou [6] [7] took the stroke direction, curvature, and bending times of the oracle-shaped drawings as secondary features and encoded them. But only experts can master this method skillfully. Gu [8] calculated the fractal dimension

of oracle bone inscriptions and matched it with the characteristic database of oracle bone inscriptions to identify oracle bone inscriptions. Liu [9] developed the oracle character recognition method based on SVM. However, due to the coexistence of complex and simplified oracle characters, the recognition accuracy can still be improved. Gao [10] presented a two-stage method of variant character recognition for oracle bone inscriptions, which used VGG16 to recognize variant characters of oracle bone inscriptions.

In the aspect of image embedding, Liang [11] attempted to use an unsupervised method to process the image content by binarization, combining the vectors of each direction into a row vector as the feature representation of the image content, but the recognition accuracy is low. In the deep learning field, Trinh [12] combined the idea of a masked language model with a transformer to achieve the unsupervised learning of image tasks, with the goal of improving ResNet-50. Faghri [13] obtained the features of images and texts through convolution and sequence networks and used GRU to map the text and image to the same subspace. Chen [14] used the manifold relation to learn image feature embedding and manifold learning to refine the distance measurement. Ren [15] used Node2Vec to generate graph embeddings of nodes and calculated user-news relevance using cosine similarity. The current research mainly uses traditional image processing ideas and finally introduces the supervised network model [16]-[18].

For the recognition of glyph images, such as handwriting identification, statistical analysis of data sets is often used to extract features and classify them. Thinning [19], binarization [20], normalization, and other methods are used in image preprocessing. In the aspect of feature extraction, researchers generally extract global static features [21], such as the writing center of text, font size, spacing, etc., in addition to moment features [22] and texture features [23]. Support vector machine and nearest neighbor algorithm are generally used in the initial classifier, but neural networks are mostly used at present.

We study the problem of oracle font recognition based on an unsupervised learning method. There were TF-IDF and subtractive clustering methods [24]-[26] for font feature extraction based on unsupervised learning. It is found that the success rate of unsupervised learning-based font feature recognition is very low with few training samples. We extract the horizontal and vertical features of the image from the image pixels and convert them into text. Using the internal correlation of the image, we realize unsupervised image recognition with high accuracy.

In this study, we proposed the model Bone2Vec (see **Figure 2**) to enable the recognition of oracle bone scripts and to test our conjecture as to whether left-handedness existed among the carvers of oracle bones more than 3000 years ago. The model Bone2Vec is divided into 3 stages. Through the experimental results, our model preliminarily empowers the identification of the font structure of oracle bone inscriptions. This method can be used in many unlabeled classification scenarios, such as the classification of ancient Mayan characters with hieroglyphic characteristics and Sumerian cuneiform characters.

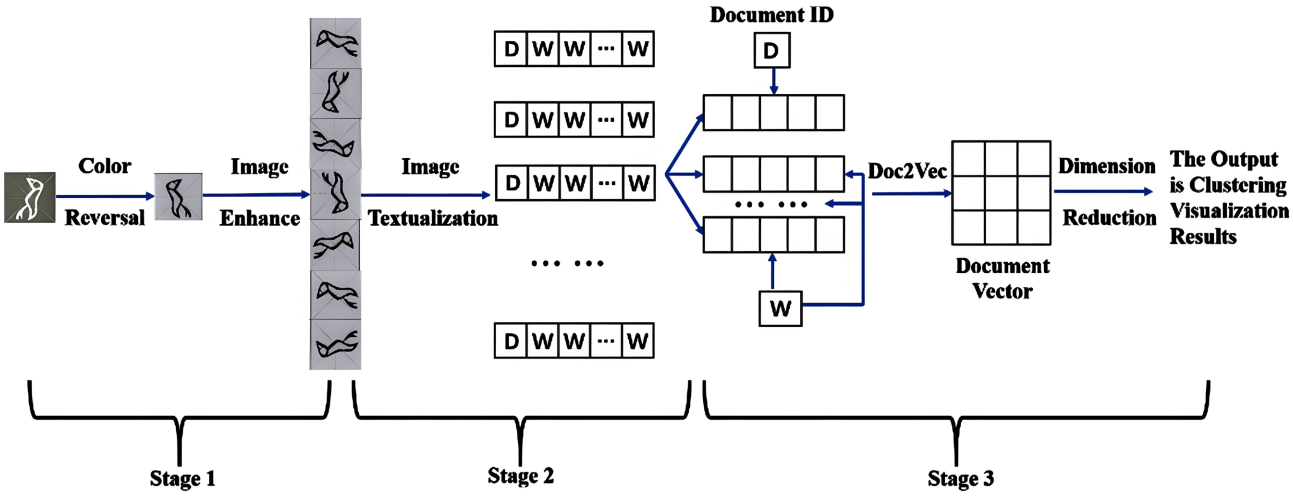

Figure 2. Three-stage Bone2Vec model.

In Figure 2, Stage 1: Given that the "age-old, data-scarce" oracle inscriptions need data enhancement, we use an image enhancement method to generate many images in line with the multiple characteristics of oracle characters to expand the training samples and improve the generalization ability of the model and the recognition ability of the oracle structure. Referring to the same character of oracle bone inscriptions with multiple morphological features, many images are generated by image enhancement. Stage 2: Image textualization. The image content mapping method is used to convert the gray value of pixels into text to realize image textualization. Our basic idea is that the gray value of each pixel in the oracle bone image is equivalent to a word in the text. The gray value of pixels in different images and the number of the same gray value are different, which corresponds to the differences in the types and frequency of words that may appear in documents with different semantics in natural language processing. These differences constitute the characteristics of images or documents. Stage 3: The image text is vectorized using the unsupervised deep learning model Doc2Vec, prior knowledge, and clustering methods are introduced to identify the oracle font structure, and the high-dimensional vectors are reduced to two dimensions through a nonlinear method to obtain clustering visualization results.

3. Methods

3.1. Image Enhancement and Textualization

In this study, the data enhancement method [27] is used to generate many related oracle bone characters automatically. Given the many forms of oracle bone inscriptions and the coexistence of positivity and negation, the mirror image writing of one part or the entire character of the oracle bone inscriptions has the same meaning. Some oracle bone inscriptions have the characteristics of left-right or upper and lower symmetry. Therefore, we can use various image enhancement methods and generate many images in line with the characteristics of oracle bone

painting. The image enhancement operations in this study depend on the task. For oracle character recognition and structure clustering, we use rotation, flipping, image size change, and vertical deformation to reflect the multiple morphological variations of oracle characters. For handedness inference, however, we exclude horizontal and vertical flipping, because these transformations may alter the visual cues related to left-or right-hand production. In that setting, only label-preserving transformations are used.

In the process of image textualization, image information must be extracted. Usually, the text image is black on a white background, while our dataset is photocopied from the original rubbings of oracle bone inscriptions, which are white on a black background. Therefore, the original image of oracle bone inscriptions obtained by scanning the entire image and segmenting the words should be color-reversed to make the text part black and the background part white. Then, graying processing is carried out for the image to contain only brightness information and no redundant color information. Thus, the image pixel content can be mapped to a simple representation of a numerical matrix. Finally, to extract the horizontal and vertical features of the image simultaneously, the image numerical and transpose matrices are spliced and stored in the document as the feature representation of the image content.

Algorithm 1 Feature extraction method of oracle bone inscriptions

Input: Image set, $\{Img\} = \{img_1, img_2, ..., img_n\}$
Output: Feature representation of oracle bone inscriptions

1: for each $img_i \in \{Img\}$ do
2: *Let* $\{result\} = 0$
3: Image graying
4: Image enhancement
5: Extract the image pixel matrix
6: Obtain the transpose matrix of the pixel matrix
7: Combined picture features
9: end for
10: return result

3.2. Word Embedding Model

Bengio [28] developed the word embedding model. Le and Mikolov [29] proposed the Word2Vec model based on the word embedding model.

Word2Vec can better express the similarity and analogy between different words. The Word2vec tool mainly contains two models (see **Figure 3**): the skip-gram model (skip-gram) and the continuous bag of words model (CBOW). These two models are the realization of the vector representation of text. The Skip-gram model uses the known current word to predict the context, and constantly adjusts the word vector of the head word by using the prediction results of the words in the context. The CBOW model is used to predict the current word through the known context, and constantly adjusts the vector of surrounding words by using the prediction result of the head word.

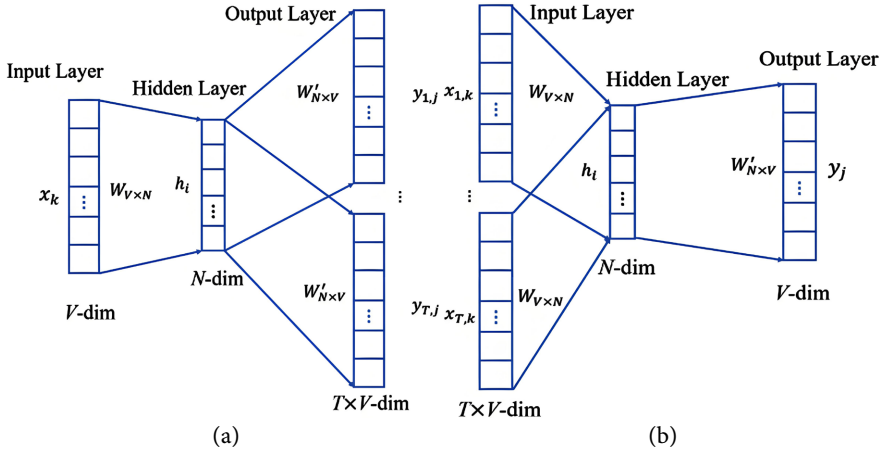

Figure 3. Main models of Word2Vec: (a) Skip-gram model; (b) CBOW model.

Doc2Vec has two kinds: Distributed Memory Model of Paragraph Vectors (PV-DM) and Distributed Bag of Words version of Paragraph Vector (PV-DBOW). We used the PV-DM algorithm presented in the document embedding model, which is based on the idea of the CBOW model.

In this framework, every word is mapped to a unique vector, represented by a column in matrix W. The column is indexed by the position of the word in the vocabulary. The concatenation or sum of the vectors is then used as features for the prediction of the next word in a sentence.

More formally, given a sequence of training words $W_1, W_2, W_3, \cdots, W_T$, the objective of the word vector model is to maximize the average log probability:

$$\frac{1}{T}\sum_{t=k}^{T-k}\log p\left(W_t \left| W_{t-k}, \cdots, W_{t+k}\right.\right). \tag{1}$$

The prediction task is typically done via a multiclass classifier, such as softmax. There, we have $P\left(W_t \left| W_{(t-k)}, \cdots, W_{(t+k)}\right.\right) = \frac{e^{y_{(W_t)}}}{\sum_i e^{(y_i)}}$ Each of y_i is un-normalized log-probability for each output word i, computed as yi

$y = b + Uh\left(W_{t-k}, W_{t-k+1}, \cdots, W_{t+k}; W\right)$ where U, b are the softmax parameters. h is constructed by a concatenation or average of word vectors extracted from W.

3.3. Image Embedding

We use the Doc2Vec document embedding model to achieve document vectorization. Doc2Vec model has been widely used in the field of word processing, but this work uses it for image vectorization. The processing of images and documents has a certain similarity. Each pixel of an image can be regarded as a word in the document, and the image matrix can be regarded as a document. The Doc2Vec model can quantify the word usage and context information in the document. Thus, this model can also identify the appearance, proximity, and arrangement of pixels in the image document. Meanwhile, considering that the model only recognizes the x-axis context, we add the transpose matrix of the image numerical ma-

trix to provide the y-axis context information when extracting the image text representation. There is no standardized note for Oracle data, and the complexity of Oracle writing makes the manual construction of the structure pattern of Oracle impossible. It is necessary to use an unsupervised method. Therefore, it is a meaningful exploration and innovation to introduce the Doc2Vec model into the unsupervised image field.

First, a feedforward neural network model $f\left(t_{m-k+1},\cdots,t_{m-1}\right)$ is constructed to fit the conditional probability of a word sequence composed of gray values. For the text sequence $S=t_1,t_2,\cdots,t_n$, the probability is expressed as

$$P\left(S\right)=P\left(t_1,t_2,\cdots,t_n\right)=\prod_{m=1}^{m=n}P\left(t_m\left|t_1,t_2,\cdots,t_{m-1}\right.\right). \tag{2}$$

In this study, the PV-DM model in Doc2Vec is used to train the space representation of the vector. In addition to all the pixel values in the oracle text, the Document ID is added in the neural network input. The Document ID is unique, and it can represent the subject word of the document. In the output, the multidimensional vector of each text can be obtained, and each dimension represents a hidden feature of the image represented by the text. These features summarize the horizontal and vertical features of the image represented by the text.

Due to the unitary invariance of the document embedding vector [30] [31], the relative position between the document embedding vectors does not change, and the geometric properties between the vectors do not change when the document embedding vector is rotated or transformed symmetrically in the geometric space. From the perspective of semantics, the transformed document embedding vector can be equivalent to the vector before the change. Given the symmetry of oracle images, Doc2Vec can process the horizontal and vertical image features after reading the image features into the text, and read the neighborhood information of image pixels. The similarity, analogy, and clustering of document embedding vectors are all part of the unitary invariance of embedding vectors. By using the clustering of the document embedding vector, the image text with similar features can be gathered to distinguish the oracle bone inscriptions.

Therefore, according to the unitary invariance of the document embedding vector and the positive and negative coexistence, and left-right symmetry of oracle bone inscriptions, the document embedding matrix can be defined as $A = MM^{\mathrm{T}}$. The document embedding matrix A and the original document embedding vector M have the same properties in the geometric space. It is a $N\times N$ matrix, and the vector in the ith row of the matrix is $V_i\left(v_{i1},v_{i2},\cdots,v_{iN}\right)$. At the same time, the image features of oracle bone inscriptions represented by the embedded matrix are consistent with the original documents.

In different dimensions and windows, the image embedding matrix is different. We proposed a loss calculation formula for image embedding, which is very simple, but provides an efficient supervision signal for learning to express feature representation, thus optimizing the parameters of image embedding. These features

can be well used in downstream prediction tasks. The loss function is defined as *Oracle_DVL*, where M_p and M_q represent two different document embedding matrices, and *Oracle_DVL* takes Euclidean_distance:

$$Oracle\_DVL\left(M_p, M_q\right) = \left\|A_p - A_q\right\| = \text{Euclidean\_distance}\left(A_p, A_q\right) \tag{3}$$

The image embedding function calculates the document embedding vectors M_p and M_q for the same document relative coordinate drift, and then offsets the dependence on a specific coordinate system.

To obtain the best effect of document embedding, the loss function of document embedding is used to determine the optimal window and dimension.

Algorithm 2 Optimal vector_size and window selection

Input: Document set{doc}
Output: Optimal vector_size and optimal sliding window for document embedding

1: Set window fixed
2: for dimension in (lower bound, upper bound):
3: M = Doc2Vec ({doc}, window, vector_size)
4: $A = MM^T$
5: {A}.append(A)
6: for A_1 in {A}:
7: SUMDVL=SUM(DVL(A_1, A_{other}))
8: {*Oracle_DVL*}.append (*Oracle_DVL*)
9: Optimal vector_size = min{*Oracle_DVL* }.dimension
10: Set dimension fixed
11: Perform steps 2 - 8
12: Optimal window = min{*Oracle_DVL* }.window

According to Algorithm 2, the control variable method is used to determine the two parameters: sliding window and model vector_size of the Doc2Vec model in turn. The running results on dataset 1 are shown in Figure 4. Therefore, we confirm the optimal dimension vector_size = 680 and optimal window = 8.

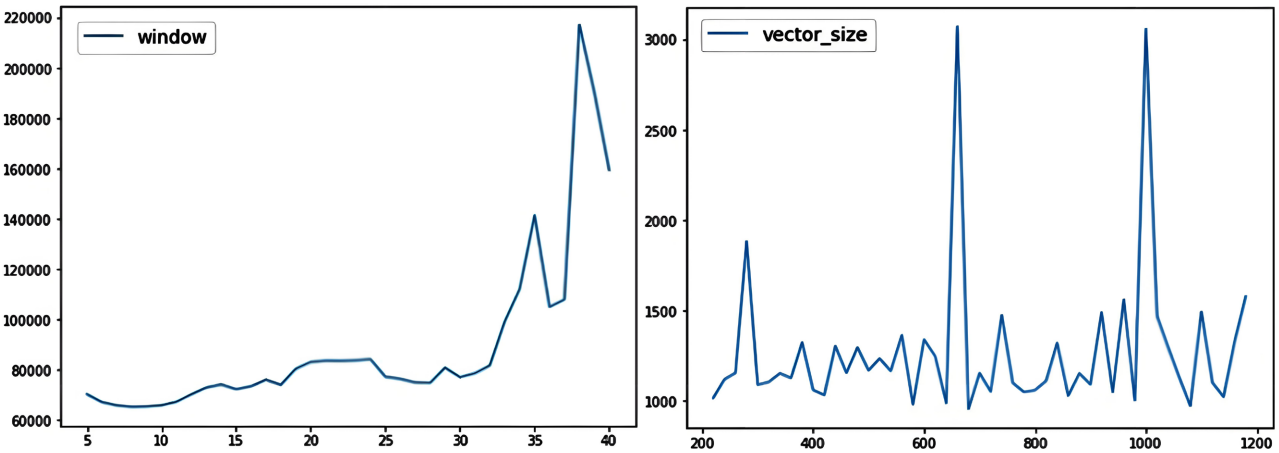

Figure 4. Determination of optimal window (a) and optimal vector_size (b).

3.4. Manifold Learning Dimension Reduction

The evaluation pipeline consists of two stages: first, oracle images are converted into document-like representations and embedded by Doc2Vec without using handedness or character labels; second, after the embeddings are obtained, labels are introduced only for downstream evaluation, where visualization and a logistic regression classifier are used to assess how well the learned representations separate the target categories.

Manifold learning dimensionality reduction is a process of finding low-dimensional data in high-dimensional spatial data, that is, mapping f for dataset $\{a_i\}$ in high-dimensional space and constructing a low-dimensional dataset $\{y_i\} = \{(a_i, b_i)\}$ where y_i satisfies the given condition in the dimension. We use the nonlinear dimensionality reduction method in manifold learning. For the document embedding matrix of high-dimensional data, we use the nonlinear dimensionality reduction method, which can retain the original features of the oracle image, and visualize the low-dimensional data. The dimension reduction of the oracle image vector can help find the structural and writing features hidden in the oracle image.

We use the T-SNE [32] dimension reduction method. It uses the gradient descent method for learning in dimension reduction to enlarge the distance between different oracle image clusters. Compared with the linear dimension reduction method, it can gather the same kind of vectors into the same cluster, and realize the two-dimensional visual clustering of oracle bone images.

For the two-dimensional manifold after dimension reduction $\{y_i\} = \{(a_i, b_i)\}$, for any two clusters Y_1 and Y_2, Y_1 has N_1 points, Y_2 has N_2 points, and the distance between the two clusters can be calculated as:

$$\begin{aligned}\text{clust\_distance}(Y_1, Y_2) &= \frac{\sum_{i=1}^{N_1}\sum_{j=1}^{N_2} dis\tan ce\left(y_i^{(1)}, y_j^{(1)}\right)}{N_1 \times N_2} \\ &= \frac{\sum_{i=1}^{N_1}\sum_{j=1}^{N_2}\sqrt{\left(a_i^{(1)} - a_j^{(1)}\right)^2 + \left(b_i^{(1)} - b_j^{(1)}\right)^2}}{N_1 \times N_2}\end{aligned}$$

The cluster distance equation can quantitatively represent the similarity between two types of documents, and then represent the similarity between the images represented by the documents. The closer the distance is, the more similar the two types of documents are. Due to the embedding vectors of image documents clustering and the distance between similar image documents being small, they tend to cluster. T-SNE dimension reduction enlarges the distance between different classes in the process of learning by the gradient descent method, which makes the visualization effect of clustering more obvious. In order to show the similarity between images more intuitively, after T-SNE dimension reduction, we used the original image to replace the point to visualize the image.

4. Results

Here we empirically investigate four datasets based on our proposed model, re-

porting both unsupervised embedding/clustering results and supervised probe-based evaluation results for oracle script recognition and handedness validation. First, we used datasets 1 and 2 to verify the effectiveness of our model, and then applied the model to identify and cluster datasets 3 and 4. Details of the data and model are presented in the section Materials and methods.

4.1. Data Preparation

There are four datasets. For transparency, we report for each dataset the number of writers, the number of character categories, the number of genuine oracle samples if applicable, and the total number of images before and after augmentation. Dataset 1 is the number 5 written in left and right hands by ten different people, with 115 pictures each. Dataset 2 is the oracle bone inscriptions written by modern people. We cut the original pictures, and there are 381 types of oracle bone inscriptions and 770 pictures. It is based on the imitation of oracle bone inscriptions by modern people. It only imitates the shape of oracle bone inscriptions, but does not consider the stroke thickness and writing style of oracle bone inscriptions. The dataset 3 is collected from the photocopied data of all the real oracle rubbings that have been identified. It is scanned, cut into single characters, and enlarged by the authors of this paper. Each image is named according to its corresponding Chinese character. The dataset is about 10 G. There are 1108 types of oracle bone characters and 4634 single-character images. It is the largest and most perfect dataset in the research of oracle bone inscriptions in the computer vision field at present. The images contain many details, such as the stroke thickness and the edge smoothness of the original oracle bone inscriptions. Dataset 4 is the "Bao" of the original oracle bone topographies copied by 4 left-handed and 4 right-handed individuals. There are 64 figures in total, 32 for each of the left and right hands.

The authors declare that all the data supporting the findings of this study are available from the corresponding authors upon reasonable request. For all classification experiments, the train/test split was performed before augmentation at the level of non-overlapping original images or writers, and augmentation was applied only to the training set. This prevents augmented versions of the same source sample from appearing in both sets.

4.2. Recognition of Left- and Right-Hand Handwritten Digit 5

First, the Bone2Vec model is constructed for dataset 1. Dataset 1 is an image set of the number 5 written by 10 modern people. Because the flexibility of modern people's fingers is much higher than that of the ancients, the use of too complex characters cannot simulate the writing state of the ancients, so a simple number 5 is selected to verify the effectiveness of the model in distinguishing left and right hands.

The images in dataset 1 are processed according to Algorithm 1 to generate image text. The optimal dimension and optimal window are used to generate the document embedding vector. The vector is normalized to get the document embedding matrix. The normalized vector of each document is manifold learned, and the T-SNE method is used to reduce the dimension and visualize. After unsupervised

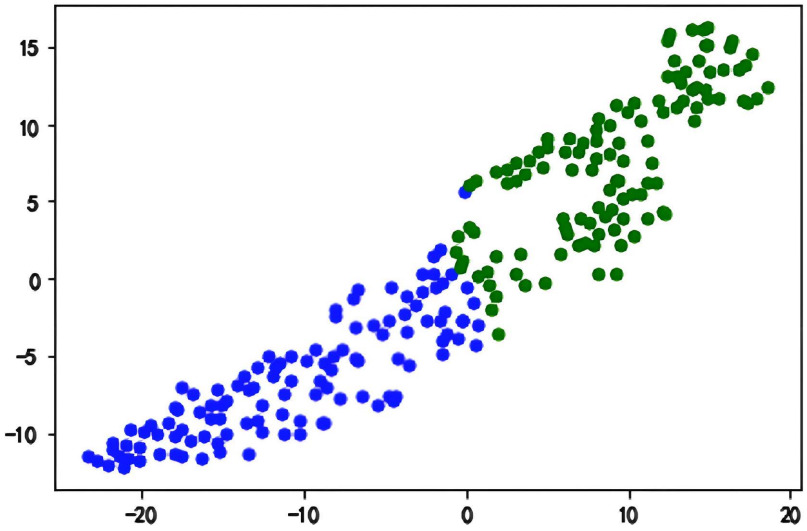

Figure 5. Visualization of left and right handwritten number 5 (blue is left-handed, and green is right-handed).

representation learning, we introduced the left-hand and right-hand labels only for evaluation. The learned embeddings were split into training and test sets, and a logistic regression classifier was trained on 60% of the data and evaluated on the remaining 40% to quantify the separability of the unsupervised representations. The classification results (**Table 1**, Experiment 1) show that the classification accuracy reaches 83%.

It can be seen from the clustering visualization results (see **Figure 5**) and classification results that the model can preliminarily distinguish the number 5 written by the left or right hand.

In order to avoid the contingency of the outcome, we carried out 10 repeated experiments, each time selecting one-third of the data from the original dataset for processing. The clustering result (see **Figure 6**) of number 5 written in left and right handwriting is good, and the Bone2Vec model can be used to distinguish the words written by left or right hand.

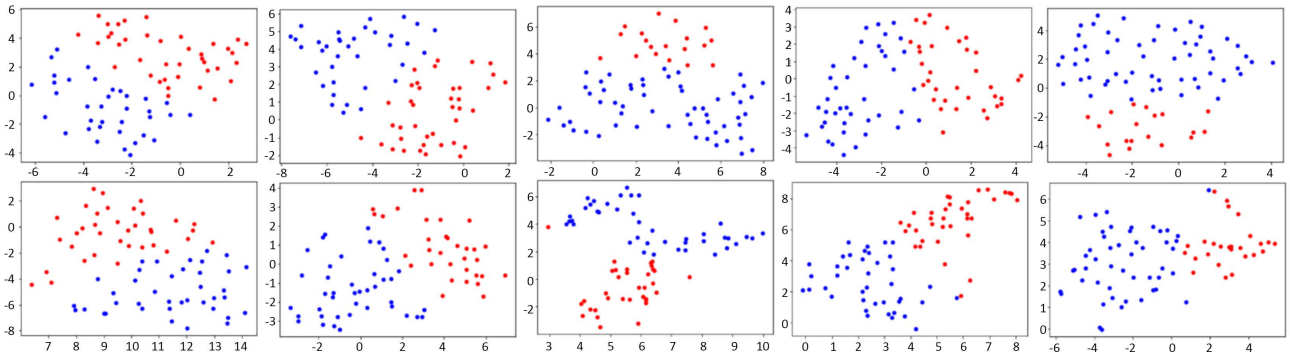

Figure 6. Results of 10 repeated experiments (blue is left-handed, and red is right-handed).

4.3. Modern Oracle Character Recognition

In order to verify the effectiveness of the model on the oracle dataset, we extracted

two oracle characters, “Bao” and “Bing”, from dataset 2, and used image enhancement to expand the dataset to 230 images, in which the characters “Bao” have 120 images and “Bing” have 130 images. Using Bone2Vec, the results are visualized as in Figure 7. After unsupervised representation learning, we introduced the oracle character labels only for evaluation. The learned embeddings were then divided into 60% training data and 40% test data, and logistic regression was used as a simple supervised probe to assess whether the unsupervised representations separate different character categories. The classification results (Table 1, Experiment 2) show that the classification accuracy reaches 88%. The algorithm can gather similar oracle characters together, which proves that the algorithm has a good effect in the recognition of the oracle font structure.

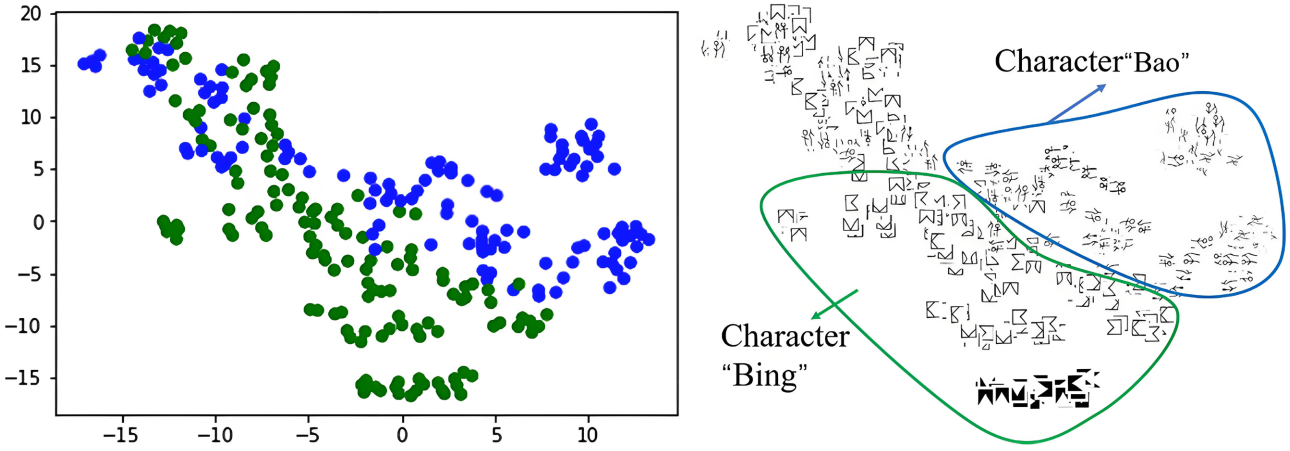

Figure 7. Visualization results of two types of oracle characters (blue is “Bao”, and green is “Bing”).

Again, to avoid the contingency of the outcome, we ran 10 replicates, each with a third of the data from the original dataset. The clustering result of Oracle (see Figure 8) is good, and the Bone2vec model can be used to distinguish Oracle characters.

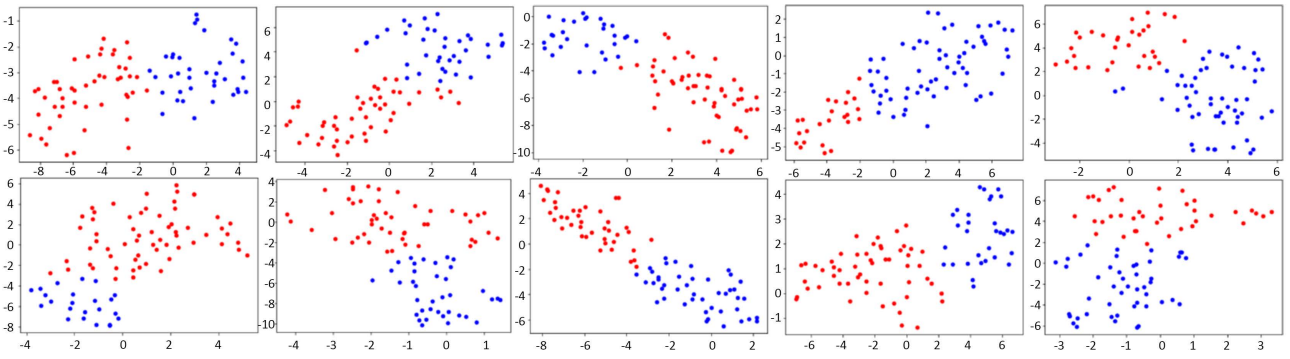

Figure 8. Visualization diagram of 10 repeated experiments of two types of oracle characters (blue is “Bao”, and red is “Bing”).

4.4. Structure Recognition of Genuine Oracle Characters

Through Experiments 1 and 2, we verified the effectiveness of Bone2Vec in the recognition of handwritten digit 5 and oracle bone inscriptions. Next, we applied

the Bone2Vec model to oracle rubbings, which come from a genuine oracle.

We have proved that Bone2Vec can extract features of oracle bone inscriptions copied by modern people. In order to prove that this method is still effective for the original image of oracle bone inscriptions, we select several groups of oracle bone inscriptions with different features. From the dimensionality reduction visualization results, the complex and simple glyphs (see **Figure 9(a)**) are nonlinearly separable, and our model can distinguish complex and simple oracle images. The similar glyphs are clustered together, while the glyphs (see **Figure 9(b)**) containing circles and cross structures are still nonlinearly separable.

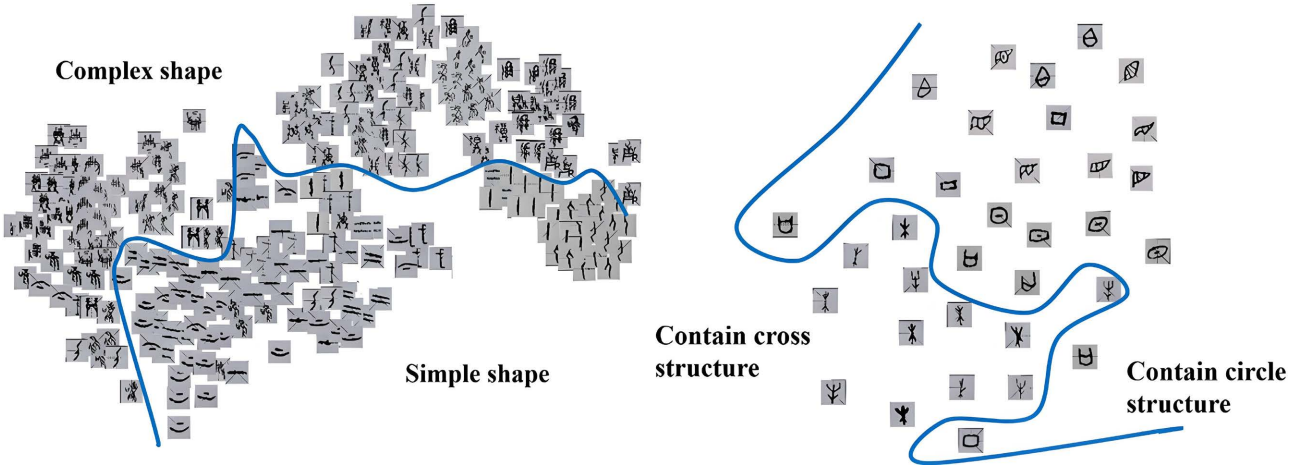

Figure 9. Visual results of partial text clustering on a real oracle bone. (a) The complex and simple glyphs are nonlinearly separable. (b) Symbols of circular and cross structures are nonlinear and separable.

Although we can see from the experimental results that our algorithm can make oracle bone inscription images with common features gather together. However, the characteristics of oracle bone inscriptions may be determined by many factors, such as the structure of the glyph, the style of the writer, the writing period, the left and right hands used by the writer, etc.

In order to verify our initial conjecture about whether there are sinistromanual or not among the seal carvers of oracle bone inscriptions, we copied several groups of oracle bone inscriptions with left and right hands respectively, and carried out several groups of experiments combined with real oracle bone images. We first collected 64 copied samples of "Bao" from modern writers in Dataset 4, including 32 left-hand samples and 32 right-hand samples, and expanded them to 512 images after data augmentation.

First, we constructed the image embedding vector from the character "Bao" data copied by our left and right hands. The clustering result (see **Figure 10(a)**) shows that the model can preliminarily distinguish the left and right handwritten text. After the unsupervised embeddings were obtained, we introduced the left-hand and right-hand labels only for evaluation. We then used logistic regression on a 60%/40% train/test split as a supervised probe of whether the learned repre-

sentation preserves handedness-related differences. The classification results (Table 1, Experiment 3) show that the classification accuracy reaches 81%, which indicates that the model has well extracted the features of the oracle bone image.

Next, we added the real oracle rubbing's image to the image we copied. After data enhancement, a total of 18 images were obtained. The real rubbings of oracle bone inscriptions are mixed with the left and right handwritten characters (see Figure 10(b)). Some of them are mixed with the left-handed characters, and some are mixed with the right-handed characters. One of the genuine oracle characters fell in the left-handed images, accounting for 5%.

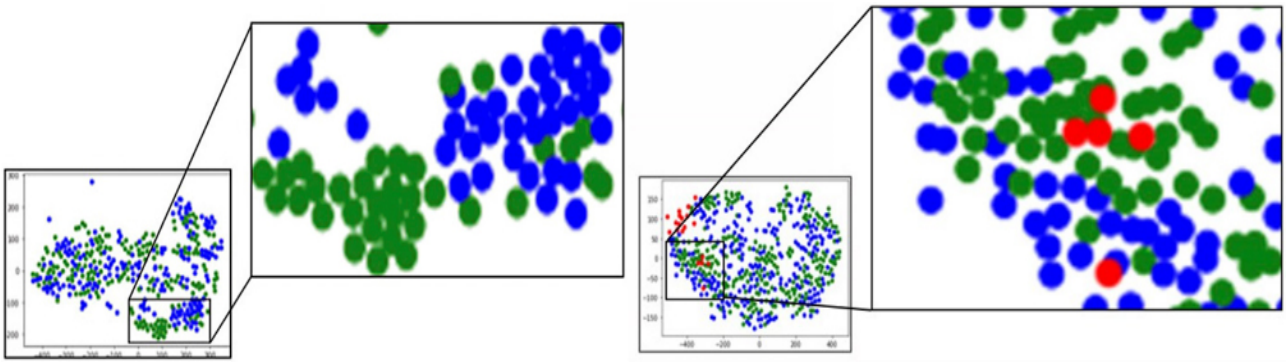

(a) (b)

Figure 10. Clustering results (blue is written by the left hand, green is written by the right hand, and red is the genuine oracle characters). (a) Only left and right handwritten "Bao". (b) The mixture of handwritten and genuine oracle characters "Bao".

We use the following inference rule: if a genuine oracle sample is embedded into the same cluster region as the modern samples produced by right-handed copying, and remains separated from the left-handed copying cluster, then the visual features captured by the model are more consistent with right-handed carving behavior than with left-handed carving behavior. Under this rule, most genuine oracle samples are associated with the right-handed cluster, which provides model-based evidence that the writers of oracle bone inscriptions were more likely to be dextromanual. Through the unsupervised adaptive graph embedding learning algorithm, we can use the computer to study and guess the production and lifestyle of ancient human beings through the recognition of ancient character images.

Table 1. Classification results of three sets of experiments.

		Precision	Recall	F1-Score	Support
Experiment 1	Left	0.85	0.82	0.84	50
	Right	0.80	0.83	0.81	42
	Accuracy	-	-	0.83	92
Experiment 2	Bao	0.89	0.85	0.87	48
	Bing	0.88	0.91	0.89	56
	Accuracy	-	-	0.88	104

Continued

	Left	0.79	0.86	0.81	109
Experiment 3	Right	0.84	0.75	0.79	96
	Accuracy	-	-	0.81	205

5. Conclusions

Oracle bone inscriptions are thus far the earliest mature writing system discovered in China and also the most widely recognized word system in the human world. From the discovery, most of the oracle words have still not been recognized, keeping their own stories from modern people.

There are difficulties in the recognition of oracle font structure using supervised deep learning because the oracle words are hard to label. As a result, unsupervised learning has to be used in our research. Yet unsupervised learning for oracle bone images is still an arduous task because genuine oracle samples do not carry explicit labels indicating whether they were carved by the left or right hand. Therefore, we introduced two reference sets produced by modern participants copying oracle forms with their left and right hands. These copied samples are used not as historical equivalents of the ancient inscriptions, but as behavioral proxies: they preserve the same basic task constraint of reproducing oracle forms while varying the hand used, allowing the model to capture hand-dependent differences in stroke organization and shape formation. The experimental results show that almost all genuine oracle images are assigned to the cluster region anchored by the modern right-handed reference samples, whereas the modern copied oracle words themselves distribute across both the right-handed and left-handed clusters. According to our inference rule, this pattern means that the visual structure of genuine oracle inscriptions is more similar to the right-handed reference behavior than to the left-handed reference behavior. Considering that most primates are right-handed, we infer that humans are accustomed to using the right hand, which may be due to species, not the result of social evolution. As more evidence comes to light, perhaps this left-right hand mystery will ultimately be unraveled.

We have also explored the classification of the Zhenren authors or sculptors' oracle characters. It is well known that each Zhenren corresponds to a unique king, and the historians use different Zhenren to differentiate the eras of the kings. The experiments provided some interesting new clues about the behavior of those legendary ancient kings, some 3000 years ago.

Clearly, the method is immune to image size and has good robustness to the language types. Subsequently, the proposed method not only works for ancient oracle works, but also can be used in the classifications of ancient Mayan character images, as well as ancient cuneiform Sumerian characters. The oracle characters, as well as Mayan characters and Sumerian characters, are symbols of ancient humans' civilization and a mirror for recognizing ourselves, and thereby are worth studying further.

Funding

This work was supported by the National Natural Science Foundation of China (62072463).

Conflicts of Interest

The authors declare no conflicts of interest regarding the publication of this paper.

References

[1] Wang, B. (2019) Oracle Bone Inscriptions Copybook. Beijing Arts and Crafts Publishing House. (In Chinese)

[2] Chen, T. (2010) Restudy on the Glyph System of Shang Oracle Bone Inscriptions. Shanghai People's Publishing House. (In Chinese)

[3] Warren, J.M. (1953) Handedness in the Rhesus Monkey. *Science*, **118**, 622-623. https://doi.org/10.1126/science.118.3073.622

[4] Finch, G. (1941) Chimpanzee Handedness. *Science*, **94**, 117-118. https://doi.org/10.1126/science.94.2431.117

[5] Tsai, L.S. and Maurer, S. (1930) "Right-Handedness" in White Rats. *Science*, **72**, 436-438. https://doi.org/10.1126/science.72.1869.436

[6] Zhou, X., Li, F. and Hua, X. (1996) Study on Computer Identification Method of Oracle. *Journal of Fudan University*, **5**, 481-486. (In Chinese)

[7] Li, F. and Zhou, X. (1996) The Graph Theory Method of Oracle Bone Inscriptions Automatic Recognition. *Journal of Electronics & Information Technology*, **S1**, 41-47. (In Chinese)

[8] Gu, S. (2018) A Method of Oracle Character Recognition Based on Fractal Geometry. *Journal of Chinese Information Processing*, **32**, 138-142. (In Chinese)

[9] Liu, G. (2018) Oracle-Bone Inscription Recognition Based on Deep Convolutional Neural Network. *Journal of Computers*, **13**, 1442-1450. https://doi.org/10.17706/jcp.13.12.1442-1450

[10] Gao, J. and Liang, X. (2020) Distinguishing Oracle Variants Based on the Isomorphism and Symmetry Invariances of Oracle-Bone Inscriptions. *IEEE Access*, **8**, 152258-152275. https://doi.org/10.1109/access.2020.3017533

[11] Liang, X. (2020) Social Computing with Artificial Intelligence. Springer.

[12] Trinh, T., Luong, M. and Le, Q. (2019) Selfie: Self-Supervised Pretraining for Image Embedding. https://arxiv.org/abs/1906.02940

[13] Faghri, F., Fleet, D., Kiros, J.R. and Fidler, S. (2018) VSE++: Improving Visual-Semantic Embeddings with Hard Negatives. *British Machine Vision Conference* 2018, *BMVC* 2018, Newcastle, 3-6 September 2018, 12.

[14] Chen, X. and Li, Y. (2020) Deep Feature Learning with Manifold Embedding for Robust Image Retrieval. *Algorithms*, **13**, Article No. 318. https://doi.org/10.3390/a13120318

[15] Ren, J., Long, J. and Xu, Z. (2019) Financial News Recommendation Based on Graph Embeddings. *Decision Support Systems*, **125**, Article ID: 113115. https://doi.org/10.1016/j.dss.2019.113115

[16] Hinton, G.E., Osindero, S. and Teh, Y. (2006) A Fast Learning Algorithm for Deep Belief Nets. *Neural Computation*, **18**, 1527-1554. https://doi.org/10.1162/neco.2006.18.7.1527

[17] Cevikalp, H., Benligiray, B. and Gerek, O.N. (2020) Semi-Supervised Robust Deep Neural Networks for Multi-Label Image Classification. *Pattern Recognition*, **100**, Article ID: 107164. https://doi.org/10.1016/j.patcog.2019.107164

[18] Marin, J., Biswas, A., Ofli, F., Hynes, N., Salvador, A., Aytar, Y., *et al.* (2021) Recipe1m+: A Dataset for Learning Cross-Modal Embeddings for Cooking Recipes and Food Images. *IEEE Transactions on Pattern Analysis and Machine Intelligence*, **43**, 187-203. https://doi.org/10.1109/tpami.2019.2927476

[19] Lin, J. and Li, J. (1996) Feature Extraction and Preprocessing of Offline Chinese Signature Verification. *Journal of Shanghai Jiaotong University*, **30**, 42-47. (In Chinese)

[20] Wang, J. and Qin, F. (2004) Design and Application of Adaptive Binary Filtering Algorithm for Gray Text Image. *Journal of Hefei University of Technology*, No. 5, 509-512. (In Chinese)

[21] Abdi, M.N. and Khemakhem, M. (2012) Arabic Writer Identification and Verification Using Template Matching Analysis of Texture. 2012 *IEEE* 12*th International Conference on Computer and Information Technology*, Chengdu, 27-29 October 2012, 592-597. https://doi.org/10.1109/cit.2012.126

[22] Darwish, A.M. and Auda, G.A. (1994) A New Composite Feature Vector for Arabic Handwritten Signature Recognition. *Proceedings of ICASSP* '94. *IEEE International Conference on Acoustics*, *Speech and Signal Processing*, Adelaide, 19-22 April 1994, II/613-II/616. https://doi.org/10.1109/icassp.1994.389581

[23] Said, H.E.S., Tan, T.N. and Baker, K.D. (2000) Personal Identification Based on Handwriting. *Pattern Recognition*, **33**, 149-160. https://doi.org/10.1016/s0031-3203(99)00006-0

[24] Singh, G. and Sundaram, S. (2015) A Subtractive Clustering Scheme for Text-Independent Online Writer Identification. 2015 13*th International Conference on Document Analysis and Recognition* (*ICDAR*), Tunis, 23-26 August 2015, 311-315. https://doi.org/10.1109/icdar.2015.7333774

[25] Shivram, A., Ramaiah, C. and Govindaraju, V. (2013) A Hierarchical Bayesian Approach to Online Writer Identification. *IET Biometrics*, **2**, 191-198. https://doi.org/10.1049/iet-bmt.2013.0017

[26] Taghavi Sangdehi, S.A. and Faez, K. (2009) Writer Identification Using Super Paramagnetic Clustering and Spatio Temporal Neural Network. In: Bayro-Corrochano, E. and Eklundh, J.-O., Eds., *Progress in Pattern Recognition*, *Image Analysis*, *Computer Vision*, *and Applications*, Springer, 669-676. https://doi.org/10.1007/978-3-642-10268-4_79

[27] Bloice, D.M., Stocker, C. and Holzinger, A. (2017) Augmentor: An Image Augmentation Library for Machine Learning. *The Journal of Open Source Software*, **2**, Article No. 432. https://doi.org/10.21105/joss.00432

[28] Bengio, Y., Ducharme, R., Vincent, P. and Janvin, C. (2003) A Neural Probabilistic Language Model. *Journal of Machine Learning Research*, **3**, 1137-1155.

[29] Le, Q. and Mikolov, T. (2014) Distributed Representations of Sentences and Documents. *Proceedings of the* 31*st International Conference on Machine Learning*, *ICML* 2014, Beijing, 21-26 June 2014, 1188-1196.

[30] Hamilton, W.L., Leskovec, J. and Jurafsky, D. (2016) Diachronic Word Embeddings Reveal Statistical Laws of Semantic Change. *Proceedings of the* 54*th Annual Meeting of the Association for Computational Linguistics*, Volume 1, 1489-1501. https://doi.org/10.18653/v1/p16-1141

[31] Yin, Z. and Shen, Y. (2018) On the Dimensionality of Word Embedding. *Advances*

in Neural Information Processing Systems 31: *Annual Conference on Neural Information Processing Systems* 2018, *NeurIPS* 2018, Montréal, 3-8 December 2018, 895-906.

[32] van der Maaten, L. and Hinton, G. (2008) Visualizing Data Using t-SNE. *Journal of Machine Learning Research*, **9**, 2579-2605.